



# Effect of 1-octanethiol as an electrolyte additive on the performance of the iron-air battery electrodes

R. D. McKerracher<sup>1</sup> · H. A. Figueredo-Rodriguez<sup>1</sup> · K. Dimogiannis<sup>1</sup> · C. Alegre<sup>2,3</sup> · N. I. Villanueva-Martinez<sup>3</sup> · M. J. Lázaro<sup>3</sup> · V. Baglio<sup>2</sup> · A. S. Aricò<sup>2</sup> · C. Ponce de León<sup>1</sup>

Received: 31 March 2020 / Revised: 9 May 2020 / Accepted: 21 June 2020  
© The Author(s) 2020

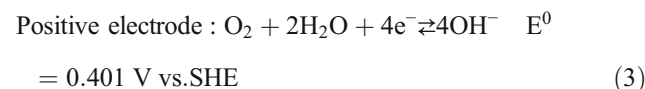
## Abstract

It has recently been established that 1-octanethiol in the electrolyte can allow iron electrodes to be discharged at higher rates. However, the effect of thiol additives on the air electrode has not yet been studied. The effect of solvated thiols on the surface positive electrode reaction is of prime importance if these are to be used in an iron-air battery. This work shows that the air-electrode catalyst is poisoned by the presence of octanethiol, with the oxygen reduction overpotential at the air electrode increasing with time of exposure to the solution and increased 1-octanethiol concentration in the range 0–0.1 mol dm<sup>-3</sup>. *Post-mortem* XPS analyses were performed over the used air electrodes suggesting the adsorption of sulphur species over the catalyst surface, reducing its performance. Therefore, although sulphur-based additives may be suitable for nickel-iron batteries, they are not recommended for iron-air batteries except in concentrations well below 10 × 10<sup>-3</sup> mol dm<sup>-3</sup>.

**Keywords** Iron-air battery · Air electrode · Iron electrode · 1-Octanethiol

## Introduction

Iron-air batteries are promising environmentally friendly battery alternatives, because iron is a widely available, low-cost, safe-to-handle, easily recycled metal [1–3]. Iron-air batteries are of particular interest, since they have a high specific energy density 764 W h kg<sup>-1</sup><sub>Fe</sub> and capacity of 1273 mA h g<sup>-1</sup><sub>Fe</sub> [4, 5]. Iron-air batteries consist of a negative iron electrode, combined with a positive air electrode that during discharge, reduces oxygen from the air. The thinness and low density of the positive electrode contribute to the high energy density of iron-air batteries. The electrochemistry of the cell is as follows:



During discharge, the iron-electrode undergoes two separate processes, firstly oxidation of metallic iron to form iron hydroxide (1), and then further oxidation to magnetite (2) or other iron oxides such as goethite, a more detailed explanation of the underlying mechanism can be found in [3, 6, 7]). The air electrode reduces oxygen obtained from the air surrounding the cell, converting it into hydroxide species (3) within the electrolyte [8, 9].

It has been established that the iron-electrode performance is limited by hydrogen evolution and electrode passivation [1, 10–17]. Adding sulphides to the electrode, the electrolyte or both, has shown to help with these problems [10, 13, 15–17]. This is because Fe-S species form on the surface of the electrode particles, improving electrode conductivity [1, 18] and inhibiting hydrogen evolution at the electrode-electrolyte interface [17]. Alkanethiols with a carbon chain length of 6–12 carbon atoms have shown to be particularly effective at inhibiting hydrogen evolution without blocking the access of

✉ H. A. Figueredo-Rodriguez  
H.A.Figueredo-Rodriguez@soton.ac.uk

<sup>1</sup> Electrochemical Engineering Laboratory, Energy Technology Research Group, Engineering Sciences and the Environment, University of Southampton, Southampton SO17 1BJ, UK

<sup>2</sup> Istituto di Tecnologie Avanzate per l'Energia, Nicola Giordano, CNR-ITAE, Salita Santa Lucia sopra Contesse, 5, 98126 Messina, Italy

<sup>3</sup> Instituto de Carboquímica, CSIC, C/. Miguel Luesma Castán, 4, 500018 Zaragoza, Spain

the electrolyte to the electrode surface [10]. Other electrolyte additives suggested have been  $K_2S$  [12, 18–21],  $Na_2S$  [16], and branched aliphatic and aromatic thiols [10, 15]. Previous research has shown that the presence of a solid sulphide additive in the electrode such as  $Bi_2S_3$ , together with an alkanethiol additive such as 1-octanethiol in the electrolyte, has a combined effect in preventing iron-electrode passivation and allowing the electrode to be cycled at higher current density rates [22].

What remains unknown at this point is the effect that electrolyte additives can have on the rest of the cell. It is important to know whether the electrolyte sulphides will affect the air electrode, and at what concentration this would happen. Previous results suggest that solid sulphides added to the iron electrode do not immediately leach out and poison the air electrode, allowing the cell to operate for some time without noticing a detrimental effect [23]. However, the effect of additives dissolved directly into the electrolyte has not been studied. In this paper, the effect of 1-octanethiol electrolyte additive on the performance of the air positive electrode is reported for the first time.

## Experimental

### Manufacture of air electrodes

The air electrodes were composed of three layers: a hydrophobic layer, catalyst layer, and current collector. They were prepared according to a method described in reference [24]. For the preparation of the hydrophobic layer, 5 g of carbon paste A (60% C, 40% PTFE) was deposited on a  $5 \times 2 \text{ cm}^2$  carbon cloth and hot-pressed at  $140 \text{ }^\circ\text{C}$  and 25 kN for 10 min, then heated in a furnace for curing at  $380 \text{ }^\circ\text{C}$  for 5 min to evaporate the remaining PTFE solvent. After the curing process, a carbon paste B (80% C, 20% PTFE) was spread over the carbon paste A, as a support layer for the catalyst ink, which was deposited evenly on top. The catalyst ink contained 50 mg of Ni-Fe hexacyanoferrate and 17 mg of composite Pd/C in 667 mg of 5 wt% Nafion solution that was sonicated for 15 min. Once the catalyst ink was dry, a  $6 \times 3 \text{ cm}^2$  nickel mesh current collector was placed against the catalyst layer and was crimped around the carbon cloth at the edges. Finally, the air electrode was hot-pressed at  $140 \text{ }^\circ\text{C}$  and 25 kN for 10 min. The resulting air electrode contained a hybrid catalyst with a loading of  $5 \text{ mg cm}^{-2}$  Ni-Fe hexacyanoferrate and  $0.5 \text{ mg cm}^{-2}$  Pd/C. The thickness of the air electrode was 0.5 mm.

### Electrolyte preparation

Electrolyte was prepared by dissolving KOH pellets to make a  $6 \text{ mol dm}^{-3}$  solution. In addition, 1-octanethiol was added to

this basic electrolyte in varying concentrations of  $0.01 \text{ mol dm}^{-3}$  and  $0.1 \text{ mol dm}^{-3}$ . No further additives were used.

### Electrochemical characterisation

The air electrodes were clamped to expose a  $1\text{-cm}^2$  area to the electrolyte in a glass cell connected to an oxygen cylinder (BOC, 99.999% purity) to supply  $100 \text{ cm}^3 \text{ min}^{-1}$  of oxygen flow into the back of the electrode. A platinum mesh counter electrode and Hg | HgO ( $1 \text{ mol dm}^{-3}$  KOH) reference electrode (+0.115 V vs. SHE) were used. The cycling of the electrodes was controlled using an Ivium n-stat potentiostat.

### Post-mortem characterisation

The air electrodes were investigated by X-ray photoelectron spectroscopy (XPS) after the performed tests. XPS was performed with an ESCA + OMICRON spectrometer with dual X-ray source ( $MgK\alpha = 1253.6 \text{ eV}$ ,  $AlK\alpha = 1486.6 \text{ eV}$ ). The deconvolution of the different peaks was carried out with the CasaXPS software considering the sensitivity factors provided by the manufacturer, Shirley background, and a 70% Gaussian/30% Lorentzian line shape [25].

## Results and discussion

### Effect of octanethiol on the cycling behaviour of the air electrode

The effect of electrolyte additives that enhance the performance of the iron electrode on the air electrode is seldomly mentioned in the literature, but other similar studies reporting the poisoning of the air electrodes in other systems such as fuel cells and other metal air batteries can be found [26–29]. Air electrodes composed of carbon cloth and nickel mesh with a layer of Ni/Fe hexacyanoferrate and Pd/C catalyst sandwiched in between were manufactured. The resulting electrodes were cycled ten times at  $20 \text{ mA cm}^{-2}$  current density in  $6 \text{ mol dm}^{-3}$  KOH electrolyte containing either no additives or  $0.01$  or  $0.1 \text{ mol dm}^{-3}$  octanethiol. The results of these cycles are shown in Fig. 1. The presence of octanethiol has little effect on the oxygen evolution potential, which remained around +0.6 V vs. Hg/HgO for all electrodes. However, the oxygen reduction potential was not stable in the octanethiol solutions. This was especially the case at an octanethiol concentration of  $0.1 \text{ mol dm}^{-3}$ , where the oxygen reduction potential decreased from  $-0.1$  to  $-0.27 \text{ V vs. Hg/HgO}$  over the 10-h period. It is likely that  $C_8H_{18}S^-$  ions are forming chemical bonds to the surface of the catalyst and blocking the access of  $O_2$  molecules.

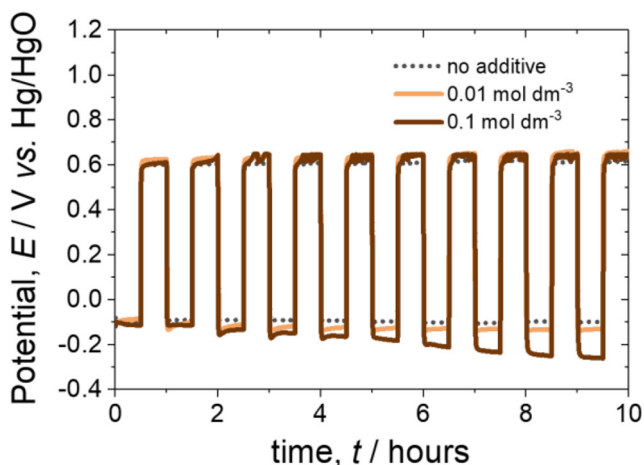


**Fig. 1** Charge/discharge profiles of the air electrode, for 1-h cycles at the current density of  $20 \text{ mA cm}^{-2}$  under oxygen flow rate of  $100 \text{ cm}^3 \text{ min}^{-1}$ , in  $6 \text{ mol dm}^{-3}$  KOH electrolyte with 0, 0.01, or  $0.1 \text{ mol dm}^{-3}$   $\text{C}_8\text{H}_{18}\text{S}$  added

Following this, fresh pieces of the air electrodes were cycled at high current densities varying from  $50$  to  $1000 \text{ mA cm}^{-2}$  to investigate the stability of oxidation and reduction potentials at the electrode in the presence of octanethiol (Fig. 2). As previously shown for this catalyst [24], the air electrode in the  $6 \text{ mol dm}^{-3}$  KOH solution showed a remarkably stable charge/discharge behaviour even at relatively high current densities ( $> 300 \text{ mA cm}^{-2}$ ). The addition of 1-octanethiol increased the oxygen reduction overpotential at the electrode for both the  $0.01$  and  $0.1 \text{ mol dm}^{-3}$  concentrations of octanethiol. The negative effect of the octanethiol was particularly evident when the current density was  $> 200 \text{ mA cm}^{-2}$ . At a current density of  $1000 \text{ mA cm}^{-2}$ , the oxygen reduction potential became highly unstable in the

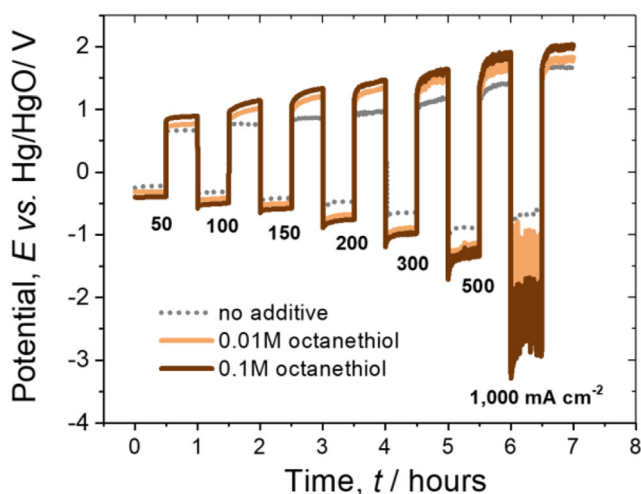


**Fig. 2** One-hour charge/discharge profiles of the air electrode, for increasing current densities of  $50$ – $1000 \text{ mA cm}^{-2}$  under oxygen flow rate of  $100 \text{ cm}^3 \text{ min}^{-1}$ , in  $6 \text{ mol dm}^{-3}$  KOH electrolyte with 0, 0.01, or  $0.1 \text{ mol dm}^{-3}$   $\text{C}_8\text{H}_{18}\text{S}$  added

solutions containing octanethiol, as shown by the electrochemical noise on the graph in Fig. 2.

In summary, it appears that at low-to-moderate current density around  $20 \text{ mA cm}^{-2}$ , octanethiol has a detrimental effect on the potential at the air electrode, which increases over time. At higher current densities, this effect is even more pronounced. A likely explanation is that octanethiol forms a self-assembled monolayer on the surface of the Ni/Fe and Pd catalysts, and on the nickel mesh current collector, in a similar way as it does on the iron electrode. *Post-mortem* XPS analyses were performed on the used air electrodes. Prior to the XPS analysis, the samples were thoroughly washed with distilled water and then dried overnight. Figure 3 shows the XPS survey for two electrodes having worked with and without 1-octanethiol. The electrode without 1-octanethiol (electrode 1 on the left) shows no sulphur on the XPS survey, whereas electrode 2 (in the presence of 1-octanethiol) presented a clear S2p peak (see Fig. 3b for detail). Considering that the XPS analysis is performed in vacuum conditions and that the electrodes were washed and dried, being 1-octanethiol a volatile substance, the presence of the S2p peak in the electrode 2 makes us infer that 1-octanethiol is adsorbed over the electrode. The sulphate peak could be an indicator of the adsorption of sulphur over nickel and/or Pd. It is known that  $\text{H}_2\text{S}$  adsorbs over Ni and, in the presence of air, oxidises to  $\text{NiSO}_4$  [30], and maybe the same could happen with mercaptans adsorbed over nickel. Besides, thiol is also known for adsorbing on both Pd and Ni surfaces [25, 31–33].

### Implications for the iron-air battery system

The strong poisoning effect of thiols at the air electrode has repercussions on the voltage stability of the cell. In a previous publication [22], we studied the performance of iron electrodes at the 0.2–2C discharge rates in the presence and absence of octanethiol at  $0.01 \text{ mol dm}^{-3}$  concentration. The same procedure repeated here at the 1C rate (corresponding to  $108 \text{ mA}$  for an iron electrode containing  $85 \text{ mg}$  of Fe) showed a marked effect of octanethiol to improve the discharge potential and discharge capacity, especially at the  $0.1 \text{ mol dm}^{-3}$  concentration Fig. 4.

If the first discharge cycles of Fig. 4 were repeated in an iron-air cell, including the air electrode from Figs. 1 and 2, the current density at the air electrode would be approximately  $100 \text{ mA cm}^{-2}$ . As can be seen by combining the potentials from Figs. 2 and 4, in an electrolyte without octanethiol, the iron-electrode first plateau discharge potential would be  $-0.68 \text{ V vs. Hg/HgO}$  and the air-electrode average discharge potential would be  $-0.24 \text{ V vs. Hg/HgO}$ , leading to a cell discharge potential of  $+0.44 \text{ V}$ . With  $0.1 \text{ mol dm}^{-3}$  octanethiol added to the electrolyte, the iron and air potentials would be  $-0.82$  and  $-0.46 \text{ V vs. Hg/HgO}$  respectively, leading to a cell discharge potential of  $+0.36 \text{ V}$ . So, although octanethiol vastly

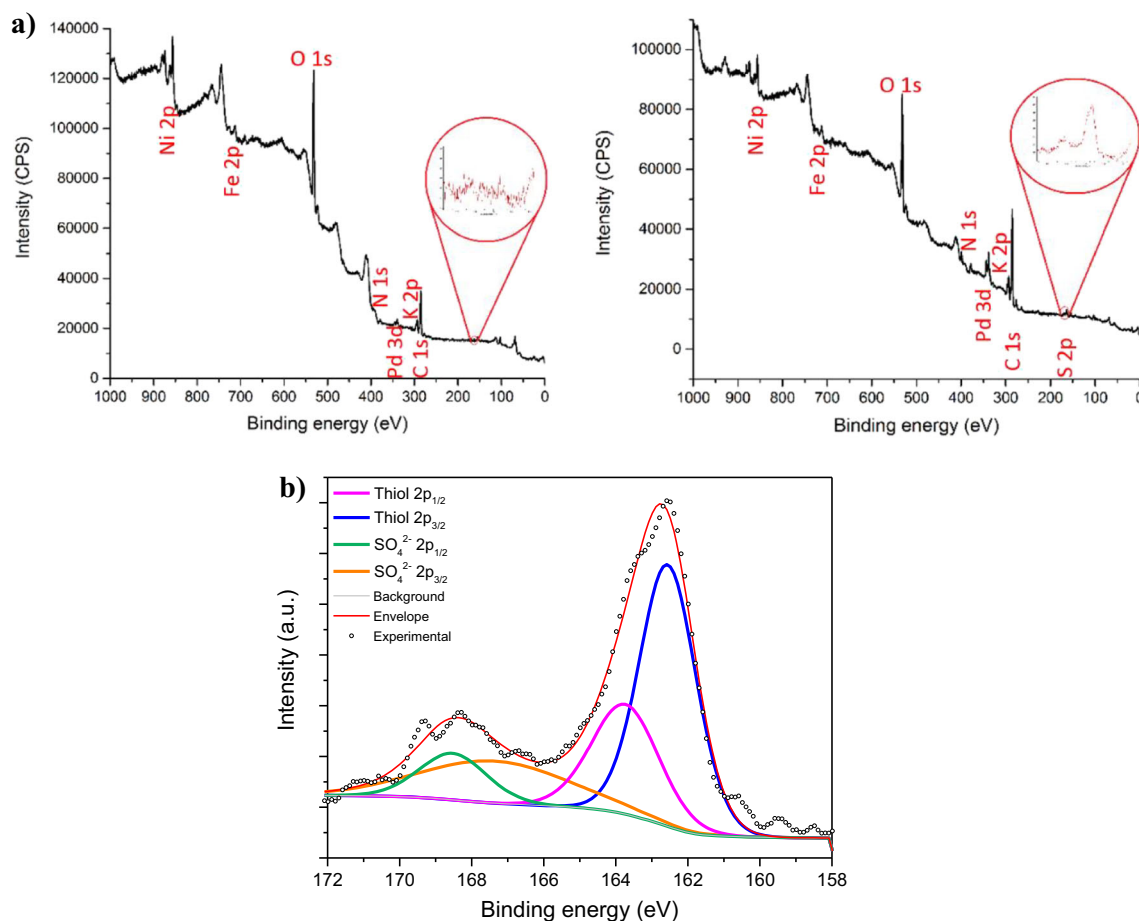


**Fig. 3** **a** XPS spectra of electrode 1 (without octanethiol) (left) and electrode 2 (with octanethiol) (right) after cycling. The inset shows a zoom of the S2p orbital. **b** High-definition XPS spectrum of sulphur in electrode 2 (with octanethiol) after cycling

improves the iron-electrode performance at high current densities, this is more than offset by a deterioration in the air-

electrode performance, which will only get worse over time (Fig. 1).

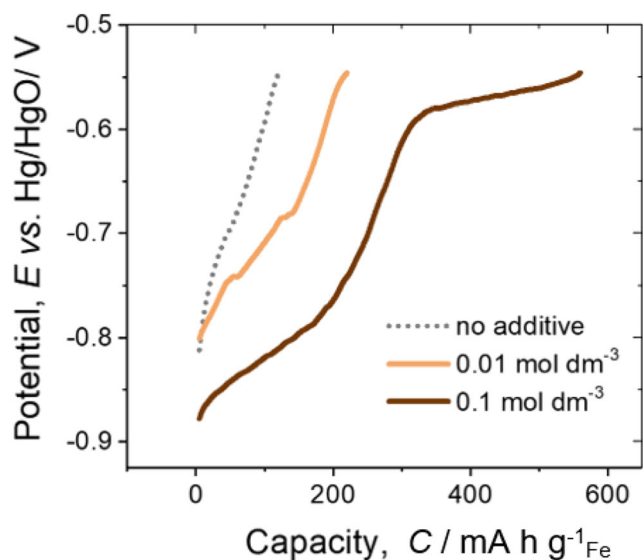


**Fig. 4** Discharge profiles for  $\text{Fe}_2\text{O}_3/\text{C}$  iron electrode (electrode produced in reference [22]) at 1C rate (108 mA), in  $6 \text{ mol dm}^{-3}$  KOH electrolyte with 0, 0.01, or  $0.1 \text{ mol dm}^{-3}$   $\text{C}_8\text{H}_{18}\text{S}$  added

## Conclusions

The use of 1-octanethiol in an iron-air cell indicates to be detrimental to the iron-air battery performance, despite its role in preventing passivation and maintaining a more negative potential at the iron electrode. The exact reason for the observed poisoning effect at the air electrode needs to be further studied. It could be attributed to the adsorbed alkanethiols or thiols that might be blocking the  $\text{O}_2$  transport to the active sites or an increment in the surface hydrophobicity. Either case seems to inhibit the catalyst performance during the ORR. This negative effect on the air electrode in the half-cell outweighs the positive influence observed on the iron electrode half-cell. Therefore, alkanethiols are not recommended as electrolyte additives in iron-air cells, especially not at concentrations  $> 0.01 \text{ mol dm}^{-3}$ . They may still be acceptable additives if used with a membrane or in other iron based such as nickel-iron batteries.

**Funding information** This work was enabled by an EU grant FP7 (NECOBAUT grant agreement no. 314159). H.A.F.R. acknowledges financial support from CONACYT, Mexico. CNR-ITAE authors acknowledge funding from the “Accordo di Programma CNR-MiSE, Gruppo tematico Sistema Elettrico Nazionale – Progetto: Sistemi elettrochimici per l’accumulo di energia”. C.A. thanks the Short-Term Mobility project of CNR and for her Juan de la Cierva contract (FJCI-2015-25560). The authors also acknowledge financial support given by Aragon Government to the Fuel Conversion Group (T06\_17R).

## Compliance with ethical standards

**Conflict of interest** The authors declare that they have no conflict of interest.

**Open Access** This article is licensed under a Creative Commons Attribution 4.0 International License, which permits use, sharing, adaptation, distribution and reproduction in any medium or format, as long as you give appropriate credit to the original author(s) and the source, provide a link to the Creative Commons licence, and indicate if changes were made. The images or other third party material in this article are included in the article's Creative Commons licence, unless indicated otherwise in a credit line to the material. If material is not included in the article's Creative Commons licence and your intended use is not permitted by statutory regulation or exceeds the permitted use, you will need to obtain permission directly from the copyright holder. To view a copy of this licence, visit <http://creativecommons.org/licenses/by/4.0/>.

## References

- Manohar AK, Yang C, Malkhandi S, Yang B, Surya Prakash GK, Narayanan SR (2012) Understanding the factors affecting the formation of carbonyl iron electrodes in rechargeable alkaline iron batteries. *J Electrochem Soc* 159(12):A2148–A2155. <https://doi.org/10.1149/2.021301jes>
- Manohar AK, Malkhandi S, Yang B, Yang C, Surya Prakash GK, Narayanan SR (2012) A high-performance rechargeable iron electrode for large-scale battery-based energy storage. *J Electrochem Soc* 159(8):A1209–A1214. <https://doi.org/10.1149/2.034208jes>
- Weinrich H, Durmus YE, Tempel H, Kungl H, Eichel RA (2019) Silicon and iron as resource-efficient anode materials for ambient-temperature metal-air batteries: a review. *Materials (Basel)* 12(13). <https://doi.org/10.3390/ma121321341-55>
- McKerracher RD, Ponce de Leon C, Wills RGA et al (2015) A review of the iron–air secondary battery for energy storage. *Chempluschem* 80(2):323–335. <https://doi.org/10.1002/cplu.201402238>
- Yang C, Manohar AK, Narayanan SR (2017) A high-performance sintered iron electrode for rechargeable alkaline batteries to enable large-scale energy storage. *J Electrochem Soc* 164(2):A418–A429. <https://doi.org/10.1149/2.1161702jes>
- Figueredo-Rodríguez HA, McKerracher RD, de León CP, Walsh FC (2019) Improvement of negative electrodes for iron-air batteries: comparison of different iron compounds as active materials. *J Electrochem Soc* 166(2):A107–A117. <https://doi.org/10.1149/2.1071816jes>
- Weinrich H, Come J, Tempel H, Kungl H, Eichel RA, Balke N (2017) Understanding the nanoscale redox-behavior of iron-anodes for rechargeable iron-air batteries. *Nano Energy* 41:706–716. <https://doi.org/10.1016/J.NANOEN.2017.10.023>
- Zhao C, Yan X, Wang G, Jin Y, du X, du W, Sun L, Ji C (2018) PdCo bimetallic nano-electrocatalyst as effective air-cathode for aqueous metal-air batteries. *Int J Hydrog Energy* 43(10):5001–5011. <https://doi.org/10.1016/J.IJHYDENE.2018.01.140>
- Alegre C, Modica E, Lo Vecchio C, Siracusano S, Aricò AS, Baglio V (2016) Pd supported on Ti-suboxides as bifunctional catalyst for air electrodes of metal-air batteries. *Int J Hydrog Energy* 41(43):19579–19586. <https://doi.org/10.1016/J.IJHYDENE.2016.03.095>
- Malkhandi S, Yang B, Manohar AK, Prakash GKS, Narayanan SR (2013) Self-assembled monolayers of *n*-alkanethiols suppress hydrogen evolution and increase the efficiency of rechargeable iron battery electrodes. *J Am Chem Soc* 135(1):347–353. <https://doi.org/10.1021/ja3095119>
- Sundar Rajan A, Ravikumar MK, Priolkar KR, Sampath S, Shukla AK (2015) Carbonyl-iron electrodes for rechargeable-iron batteries. *Electrochem Energy Technol* 1(1):2–9. <https://doi.org/10.2478/eetech-2014-0002>
- Gil Posada JO, Hall PJ (2014) Post-hoc comparisons among iron electrode formulations based on bismuth, bismuth sulphide, iron sulphide, and potassium sulphide under strong alkaline conditions. *J Power Sources* 268:810–815. <https://doi.org/10.1016/j.jpowsour.2014.06.126>
- Posada JOG, Hall PJ (2015) The effect of electrolyte additives on the performance of iron based anodes for NiFe cells. *J Electrochem Soc* 162(10):A2036–A2043. <https://doi.org/10.1149/2.0451510jes>
- Posada JOG, Hall PJ (2016) Towards the development of safe and commercially viable nickel-iron batteries: improvements to Coulombic efficiency at high iron sulphide electrode formulations. *J Appl Electrochem* 46(4):451–458. <https://doi.org/10.1007/s10800-015-0911-3>
- Yang B, Malkhandi S, Manohar AK, Surya Prakash GK, Narayanan SR (2014) Organo-sulfur molecules enable iron-based battery electrodes to meet the challenges of large-scale electrical energy storage. *Energy Environ Sci* 7(8):2753–2763. <https://doi.org/10.1039/C4EE01454E>
- Manohar AK, Yang C, Narayanan SR (2015) The role of sulfide additives in achieving long cycle life rechargeable iron electrodes in alkaline batteries. *J Electrochem Soc* 162(9):A1864–A1872. <https://doi.org/10.1149/2.0741509jes>
- Manohar AK, Yang C, Malkhandi S, Prakash GKS, Narayanan SR (2013) Enhancing the performance of the rechargeable iron electrode in alkaline batteries with bismuth oxide and iron sulfide additives. *J Electrochem Soc* 160(11):A2078–A2084. <https://doi.org/10.1149/2.066311jes>
- Hang BT, Yoon S-H, Okada S, Yamaki J (2007) Effect of metal-sulfide additives on electrochemical properties of nano-sized Fe<sub>2</sub>O<sub>3</sub>-loaded carbon for Fe/air battery anodes. *J Power Sources* 168(2):522–532. <https://doi.org/10.1016/J.JPOWSOUR.2007.02.067>
- Hang BT, Thang DH (2016) Effect of additives on the electrochemical properties of Fe<sub>2</sub>O<sub>3</sub>/C nanocomposite for Fe/air battery anode. *J Electroanal Chem* 762:59–65. <https://doi.org/10.1016/j.jelechem.2015.12.012>
- Hang BT, Watanabe T, Egashira M, Watanabe I, Okada S, Yamaki JI (2006) The effect of additives on the electrochemical properties of Fe/C composite for Fe/air battery anode. *J Power Sources* 155(2):461–469. <https://doi.org/10.1016/J.JPOWSOUR.2005.04.010>
- Kitamura H, Zhao L, Hang BT, Okada S, Yamaki JI (2012) Effect of charge current density on electrochemical performance of Fe/C electrodes in alkaline solutions. *J Electrochem Soc* 159(6):A720–A724. <https://doi.org/10.1149/2.049206jes>
- McKerracher RD, Figueredo-Rodríguez HA, Alegre C et al (2019) Improving the stability and discharge capacity of nanostructured Fe<sub>2</sub>O<sub>3</sub>/C anodes for iron-air batteries and investigation of 1-octanethiol as an electrolyte additive. *Electrochim Acta* 318:625–634. <https://doi.org/10.1016/j.electacta.2019.06.043>
- Figueredo-Rodríguez HA, McKerracher RD, Insausti M et al (2017) A rechargeable, aqueous iron air battery with nanostructured

- electrodes capable of high energy density operation. *J Electrochem Soc* 164(6):A1148–A1157. <https://doi.org/10.1149/2.0711706jes>
24. McKerracher RD, Figueredo-Rodríguez HA, Avila-Alejo JO et al (2018) A comparison of Pd/C, perovskite, and Ni-Fe hexacyanoferrate bifunctional oxygen catalysts, at different loadings and catalyst layer thicknesses on an oxygen gas diffusion electrode. *J Electrochem Soc* 165(7):A1254–A1262. <https://doi.org/10.1149/2.0321807jes>
  25. Moulder JF, Chastain J (1992) Handbook of X-ray photoelectron spectroscopy: a reference book of standard spectra for identification and interpretation of XPS data. Perkin-Elmer Corporation, Physical Electronics Division
  26. Kushi T (2017) Effects of sulfur poisoning on degradation phenomena in oxygen electrodes of solid oxide electrolysis cells and solid oxide fuel cells. *Int J Hydrog Energy* 42(15):9396–9405. <https://doi.org/10.1016/j.ijhydene.2017.01.151>
  27. Oh I, Biggin ME, Gewirth AA (2000) Poisoning the active site of electrochemical reduction of dioxygen on metal monolayer modified electrode surfaces. *Langmuir* 16(3):1397–1406. <https://doi.org/10.1021/la991005g>
  28. Xu X, Hui KS, Dinh DA, Hui KN, Wang H (2019) Recent advances in hybrid sodium–air batteries. *Mater Horizons* 6(7):1306–1335. <https://doi.org/10.1039/C8MH01375F>
  29. Muglali MI, Erbe A, Chen Y, Barth C, Koelsch P, Rohwerder M (2013) Modulation of electrochemical hydrogen evolution rate by araliphatic thiol monolayers on gold. *Electrochim Acta* 90:17–26. <https://doi.org/10.1016/j.electacta.2012.11.116>
  30. Struis RPWJ, Schildhauer TJ, Czekaj I, Janousch M, Biollaz SMA, Ludwig C (2009) Sulphur poisoning of Ni catalysts in the SNG production from biomass: a TPO/XPS/XAS study. *Appl Catal A Gen* 362(1–2):121–128. <https://doi.org/10.1016/j.apcata.2009.04.030>
  31. Kumar G, Van Cleve T, Park J et al (2018) Thermodynamics of alkanethiol self-assembled monolayer assembly on Pd surfaces. *Langmuir* 34(22):6346–6357. <https://doi.org/10.1021/acs.langmuir.7b04351>
  32. Behyan S, Hu Y, Urquhart SG (2011) Sulfur 1 s near-edge x-ray absorption fine structure (NEXAFS) of thiol and thioether compounds. *J Chem Phys* 134(24):244304. <https://doi.org/10.1063/1.3602218>
  33. Corthey G, Rubert AA, Benitez GA et al (2009) Electrochemical and X-ray photoelectron spectroscopy characterization of alkanethiols adsorbed on palladium surfaces. *J Phys Chem C* 113(16):6735–6742. <https://doi.org/10.1021/jp9001077>

**Publisher's note** Springer Nature remains neutral with regard to jurisdictional claims in published maps and institutional affiliations.